

# Temperature fiber-optic point sensors: Commercial technologies and industrial applications

Éric Pinet, Sébastien Ellyson and Frédéric Borne  
FISO Technologies

**Abstract** – Temperature fiber-optic point-sensors have been commercialized for about two decades. Among the various available optical sensing technologies, only few ones have lead to commercial successes. For instance, temperature could be measured by fluorescence decay time of a phosphorus compound excited with UV light; the higher the temperature, the faster the decay. Semiconductor band-gap thermal properties could also be used for temperature sensing. As an example for GaAs, the wavelengths transmission cut-off is increasing al linearly with temperature ( $\sim 0.3 \text{ nm}/^\circ\text{C}$ ). By analyzing with a spectrometer the reflected spectrum of a white-light source, temperature could be deduced. Interferometry-based technology such as Fabry-Pérot is also a field-proven method for accurate measurement of temperature in various applications. In this case, the optical path of a Fabry-Pérot cavity is changing with temperature ( $\sim 20 \text{ nm}/^\circ\text{C}$ ). Finally with fiber Bragg grating technology, a Bragg grating is written inside the fiber and reflects a given wavelength which is slightly shifting with temperature ( $\sim 10 \text{ pm}/^\circ\text{C}$ ).

Several industrial applications involving temperature measurement contributed to the development of commercial optical fiber sensing technologies. Those include for instance the real-time temperature monitoring of hot spots in high-power transformers, of semiconductor plasma etchers or of microwave chemical reactors. Applications in the food industry or in the medical field are now also appearing.

## 1 INTRODUCTION

Since now about two decades, optical fiber sensors [1-4] (OFS) left academic research laboratories to enter the real industrial world. Several companies started to commercialize such sensors with however a slower than expected market penetration. Being more expensive than conventional technologies, OFS were confined to usually low-volume niche applications where they remained the only possible choice.

Among the various available technologies, point-sensing as opposed to quasi- or fully-distributed OFS was probably the most successful in terms of sold units. For such sensors, the sensing element is typically positioned at or near the end of an optical fiber used as a link between the sensing element and the light source/interrogator. Point-sensors are particularly well-adapted for applications where only a limited number of measuring points are needed, typically 1 to 10. Over 10-20 measuring points, multiplexing interrogation OFS technologies are often financially or technically more interesting since a same optical fiber (or channel) could be used to interrogate a lot of different sensing locations. Such multiplexing OFS interrogators are however usually much more expensive than single-point modules, they are thus often only considered in expensive projects such as for instance in civil engineering structures instrumentation where their cost

investment represents only a small fraction of the overall project.

Since there are however a lot of industrial applications requiring only limited number of measuring locations, single-point OFS technologies were able to find interesting niche markets that could be developed thanks to the unique advantages provided by the use of optical fiber connecting the measuring location to the interrogating unit. Among the most important ones, total immunity to any electromagnetic interferences (EMI) such as radio frequency (RF) or microwaves (MW) is probably the first to come to mind as it clearly differentiates OFS to their electrical less expensive and well-established counterparts. The fact that OFS provides a truly intrinsically safe sensing measurement is certainly another key advantage in applications with explosions risks such as in the oil and gas or chemical industries. The chemical and thermal resistance of OFS is also noticeable for applications with environments too harsh for electronic sensors. Finally the miniature size ( $< 1 \text{ mm}$ ) of packaged industrial OFS temperature sensors is probably also one important technological advantage since miniature shielded electrical sensors are usually more expensive.

The purpose of this paper is to present some point-sensing OFS technologies currently well-accepted in the industry for measuring temperature. Selected industrial applications where such sensors provide a competitive advantage are also described.

## 2 COMMERCIAL TECHNOLOGIES

Several optical point-sensing technologies are now commercially available, especially for temperature sensing which is probably the most widely spread OFS in the industry: applications range from industrial process control, energy, civil engineering to medical [5-7]. Although many concepts could be used to design an optical temperature sensor [8], there are presently only four main OFS technologies that dominate temperature point-sensing:

- Fluorescence decay
- Semi-conductor band-gap variation
- Fabry-Pérot interferometry
- Fiber Bragg grating

### 2.1 Fluorescence decay temperature sensor

In fluorescence decay technology, a fluorescent compound (typically phosphorus-based although other options are possible [9]) is assembled and protected usually at the tip of an optical fiber (or could be part of the fiber itself [10]). The compound is excited with high energy short light pulses typically selected in the ultra-violet (UV) region (usually 400-420 nm). As shown at the top of Figure 1 describing fluorescence decay technology, such quantum energy moves electrons of the ground state to excited states where they move more or less rapidly depending on temperature to lower energy excitation states from which they can return to the ground state by emitting lower energy light quanta (usually in the 500-600 nm region). Such emitted light is partially captured by the multimode optical fiber, returned to the interrogator and detected with a cheap silicon broadband light detector such as photodiode or phototransistor. In order to be able collect as much reflected light as possible, very large core optical fibers are typically used. For applications where temperatures do not exceed 70°C, for instance in the medical field,  $\varnothing$  0.25-1 mm plastic optical fibers (POF) could advantageously be used. For higher temperatures, silica-based multimode optical fibers [11] or even sapphire-tipped probe [12] are preferred.

When measured over time, the light intensity could be separated in two distinct phases as shown at the bottom of Figure 1: after an intense reflected excitation pulse (at  $t_0$ ), decreasing emitted light could be recorded between  $t_1$  and  $t_2$  to be able to calculate the fluorescent decay time ( $\tau$ ) without being fooled by reflected excitation pulse. Such first-order exponential decay time, typically in the 1-4 ms range, is directly linked to the temperature seen by the fluorescent compound: the higher the temperature, the faster the decay. Since such technology is based on time-dependent light intensity

measurements, optical losses induced in the fiber, such as the ones due to bending which is more important for large core fibers, should be evaluated in order to have a more robust measurement. The intensity of the reflected excitation pulse could be used for that purpose, assuming that such reference intensity remains more or less constant between two pulses, which is often the case since acquisition rate is typically 1-4 Hz per channel. Due to the way the optical signal is obtained and processed, it is hard for this technology to achieve faster acquisition rates, which is a limitation for applications where a fast temperature feedback is required.

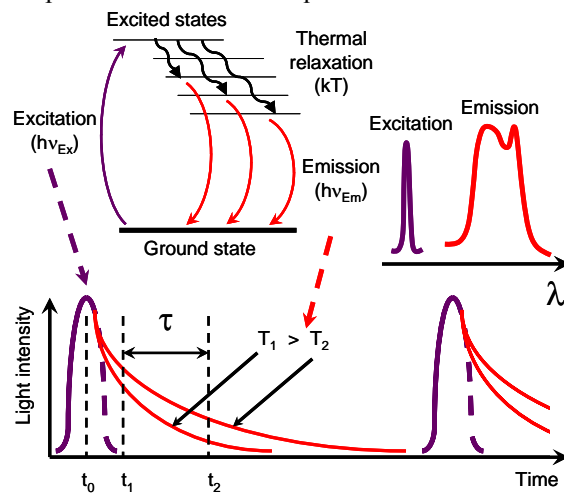


Figure 1: Schematic description of the fluorescence decay technology. Electronic transitions (top left), typical excitation and emission spectra (top right), reflected light intensity with time (bottom).

The precision that could be obtained by fluorescence decay technology is highly dependent on the selected fluorescent compound (its electronic properties, thermal resistance and stability...) but it is also related to the sensor design [13] and to the way the data is processed [14]. A typical  $\pm 2^\circ\text{C}$  accuracy is usually available for temperatures ranging from about  $-30^\circ\text{C}$  to  $+200^\circ\text{C}$  which is suitable for several industrial applications. If the temperatures range is reduced and stays within about  $20^\circ\text{C}$  of a reference calibration point, the accuracy could however be reduced to more or less one order of magnitude.

Such fluorescence decay technology, which has been on the market for now more than 15 years, has the main advantage of offering a low-cost interrogator. In its simplest version, optical interface could be limited to a UV light emitting photodiode (LED) and a silicon photo-detector placed at  $90^\circ$  in front of a 50/50 separating plate facing the optical connector of the fluorescent temperature OFS.

## 2.2 Semiconductor band-gap temperature sensor

In the semiconductor band-gap technology, a semiconductor small chip terminated by a mirror layer is glued at the tip of a multimode optical fiber. Several semiconductors could theoretically be used but practically, GaAs is the only one which has been successfully commercialized for more than 15 years.

A continuous broadband light source (such as halogen light bulb) is used to illuminate the semiconductor chip through the multimode fiber. Photons with sufficient energy could be absorbed by elastic collision with electrons of the valence band that are thus allowed to jump to the conduction band. Both bands are separated by an energy gap ( $E_g$  expressed in eV) which of course depends on the semi-conductor structure, but also on hydrostatic pressure and on temperature as show by equations (1) and (2) respectively [15]:

$$E_g(P) = E_g(0) + b \cdot P - c \cdot P^2 \quad (1)$$

where  $P$  is pressure in GPa, and for GaAs at 300 K,  $E_g(0) = 1.43 \pm 0.01$  eV,  $b = (10.8 \pm 0.3) \cdot 10^{-2}$  eV/GPa and  $c = (14 \pm 2) \cdot 10^{-4}$  eV/GPa<sup>2</sup>.

$$E_g(T) = E_g(0) - \frac{\alpha \cdot T^2}{\beta + T} \quad (2)$$

where  $T$  is temperature in K ( $0 \text{ K} < T < 10^3 \text{ K}$ ), and for GaAs at normal pressure,  $E_g(0) = 1.519$  eV,  $\alpha = 0.541 \cdot 10^{-3}$  eV/K and  $\beta = 204$  K.

In fact hydrostatic pressure does not affect much the energy gap as opposed to temperature, as a simple calculation could demonstrate. For instance assuming a pressure variation  $\Delta P$  of 1 atm from normal pressure (which is an important pressure variation for most industrial applications), the energy gap will increase by only  $\Delta E_g = 1.1 \cdot 10^{-5}$  eV. Now if we consider a temperature variation  $\Delta T$  of only 20 K increasing from 300 K, the energy gap will show a much more important decrease (about 3 orders of magnitude higher,  $\Delta E_g = -9.1 \cdot 10^{-3}$  eV).

When the semiconductor is illuminated with continuous broadband light, photons could interact with valence electrons depending on their energy given by equation:

$$E_\gamma(\lambda) = \frac{h \cdot c}{e \cdot \lambda} \approx \frac{1239.84}{\lambda} \quad (3)$$

where  $E_\gamma$  is photon energy in eV,  $\lambda$  is the photon wavelength in nm,  $h$  is the Planck constant,  $c$  is the light velocity in vacuum and  $e$  is the absolute value of the electron elementary charge.

High energy photons (lower wavelengths) will be absorbed approximately when  $E_\gamma > E_g$ . Photons with lower energy (higher wavelengths) will simply pass

through the semiconductor and be returned to the optical fiber after a reflection on the mirror capping the chip. As a result, the light returned to the interrogator will have in wavelengths the form of a high-pass filter as shown in Figure 2. Since the energy band-gap ( $E_g$ ) is mostly dependent on temperature as shown by equation (2), the position of the wavelengths cut-off is also temperature dependent. The light returned to the interrogator (which acts then as a low-resolution spectrometer) is wavelength spread geometrically over a charge coupled detector (CCD) and the wavelengths cut-off position is then evaluated by signal processing in order to determine the corresponding temperature seen by the sensor.

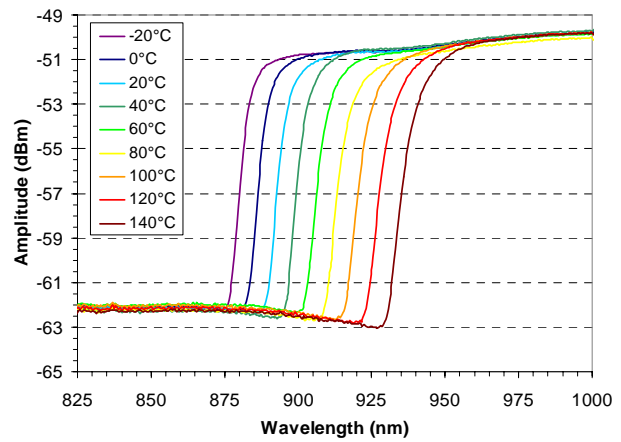


Figure 2: Reflected spectrum of GaAs sensor measured with an OSA for temperatures from  $-20^\circ\text{C}$  to  $+140^\circ\text{C}$  in  $20^\circ\text{C}$  steps.

Figure 2 shows the experimental spectral distribution obtained with an optical spectrum analyzer (OSA) of the light reflected on a GaAs chip mounted at the tip an optical fiber for temperatures ranging from  $-20^\circ\text{C}$  to  $+140^\circ\text{C}$  with  $20^\circ\text{C}$  temperature steps. It could be seen on that figure that the reflected cut-off curves are almost equally spaced meaning that their position varies nearly linearly with temperature. Actually equation (2) could be better approximated by a polynomial fit rather than by a linear fit which would give a variation of about  $0.3 \text{ nm}/^\circ\text{C}$  over the useful range of the sensor (typically from  $-50^\circ\text{C}$  to  $+250^\circ\text{C}$ ).

If we calculate the energy gap at  $-20^\circ\text{C}$  using equation (2) we obtain  $E_g(253.16 \text{ K}) = 1.443$  eV. From equation (3) it could be deduced that the corresponding wavelength cut-off should be about  $859 \text{ nm}$ . Experimentally it is actually about  $875 \text{ nm}$  (first left curve on Figure 2) showing that considerations additional to band-gap energy transfer are involved. Among the ones that should be cited, the temperature dependence of semiconductor

refractive index ( $n$ ) should be taken into account. For GaAs, it is following equation [15]:

$$n(T) = 3.255 \cdot (1 + 4.5 \cdot 10^{-5} \cdot T) \quad (4)$$

where  $T$  is the temperature in K.

However even with temperature dependence correction of the GaAs refractive index, the experimental cut-off wavelength could not precisely be calculated. With the previous example at  $-20^\circ\text{C}$ , the correction would increase the cut-off wavelength to 869 nm. Other phenomena such as other electronic transitions or local effects of ionic distribution could explain the remaining difference but it is beyond the scope of this paper.

One big advantage of the band-gap technology is the fact that the evaluation of temperature is actually wavelength dependent instead of intensity dependent. Intensity light fluctuations due to lamp aging or to fiber bending are therefore not affecting the accuracy of the measurement. Another interesting advantage is the temperature dependent wavelengths cut-off which is only related to the semiconductor properties and the sensor chip design. Once the interrogator has been calibrated to link CCD pixels position of wavelengths cut-off to actual temperature, the band-gap temperature sensors do not theoretically need any specific calibration factor. This reduces the manufacturing cost of such sensors since sensor temperature calibration is often time consuming. Typically the precision obtained for such sensor stays around  $\pm 1\text{-}2^\circ\text{C}$  for most sensors available on the market. Better accuracy of less than one order of magnitude is however always possible when specific calibration is an option.

As far as accuracy is concerned, this technology is

more or less similar to fluorescence decay previously described, and due to packaging design considerations, both technologies are often competing on similar applications. However when faster acquisition rate are required, the GaAs is superior since the signal could be continuously processed whereas for fluorescence decay it is triggered by excitation pulses frequency which could not be reduced since limited by emission relaxation processes. Typically for GaAs, acquisition rate from 4-75 Hz are presently commercially available. *FISO Technologies* will also release soon a 125 Hz GaAs interrogator in order to offer a more interesting product suitable for medical applications where faster acquisition rates are necessary.

### 2.3 Fabry-Pérot temperature sensor

The Fabry-Pérot (F-P) interferometry could be used to point-measure many different physical parameters including temperature but also pressure, strain, displacement or refractive index [16]. The principle behind this patented technology using white-light interferometry [17, 18] is sketched in Figure 3. In few words, a continuous broadband light source is injected into an optical fiber and lead to its tip where the F-P sensor is assembled. Such sensing element is made of two parallel semi-reflecting mirrors separated by a gap. The light passing through the first mirror is reflected back and forth a very large number of times between the two parallel planes forming the F-P interferometer as shown in Figure 3 (right). The light emerging from the interferometer travels back to the interrogator through the optical fiber where, thanks to a  $2 \times 2$  coupler, it is redirected to an optical analyzer and projected over a linear

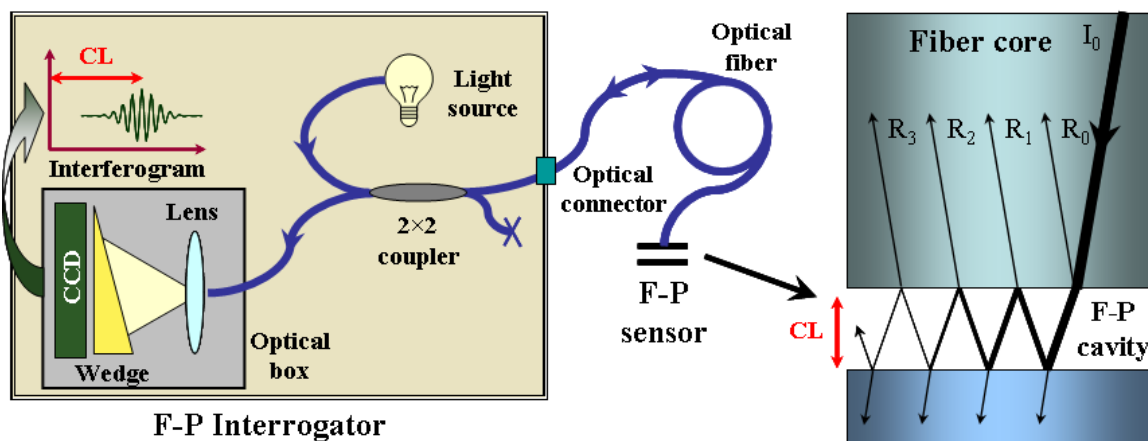


Figure 3: Schematic description of the F-P absolute measurement signal conditioner from *FISO Technologies* using patented white-light interferometry (left) and detail of F-P sensing interferometer showing ray traces obtained from a selected incident angle light beam propagating in the optical fiber core (right).

CCD detector behind a Fizeau wedge. This last interferometric device reconstructs spatially the interference pattern. Due to the fact that white-light is used, all wavelengths are present and thus destructive interferences occur except for the zero order where all wavelengths are actually constructive. Thanks to the wedge that creates a linear variation of thicknesses, the cross-correlated interference pattern has a maximum intensity at the exact position where the optical path difference (OPD) equals the one created at the F-P sensor, and few lower intensity peaks symmetrically disposed around the central peak (as given by the interferometer cross-correlation function). Thus finding the sensor OPD related to the physical parameter to be measured simply consists of finding the position of the maximum peak in the CCD interference pattern (see interferogram of Figure 3).

This robust technology, commercialized by *FISO Technologies* since 1994, allows accurate and precise F-P cavity length measurement with sub-nanometer range precision over several decades of micrometer span, thus giving a very interesting dynamical range.

The greatest advantage of this interferometric equipment, beside the fact that it is suitable for sensing various physical parameters, is that the measurement is truly absolute which means that the sensor could be disconnected and reconnected and still give the same reading without any adjustment or referencing. Due to light source and detector limitations, such technology allows also sampling rates in the  $\sim 10$  Hz to kHz ranges which are compatible with most demanding practical applications (the recently released FPI-HS from *FISO Technologies* allows a 15 kHz sampling rate). Another patented [19] relative measurement F-P interrogating technology offering an acquisition rate of 0.2 MHz (2 MHz if data post processing is possible) is also available commercially [18]. Such very high acquisition rate is rarely needed for temperature applications but is very useful for monitoring pressure in very fast occurring events such as explosions or blasts [20].

Two types of F-P temperature point-sensors are available commercially: capillary type and refractive index type. Both types are actually affecting the OPD differently: in the first, the cavity length (CL) of the F-P sensor is temperature dependent, whereas for the second, this is mainly the refractive index of the F-P sensor that contributes mostly to the OPD change with temperature.

The design of the capillary type temperature sensor consists basically on two flat-ended glass fibers that are assembled in a quartz capillary tube to form a F-P cavity. The material of one fiber is selected to have a high coefficient of thermal expansion (CTE). As the temperature increases, this fiber expands and

as a result, reduces the F-P cavity length separating the two fiber end-faces (with a thermal expansion of typically  $\sim 20$  nm/°C). Thanks to factory calibration, this length variation is translated into temperature value.

In order also to avoid that external strain could be transmitted to the sensing capillary tube, this one is encapsulated into a bigger tube. Several packaging and thermal ranges are available for such sensors and could be selected depending on the specific needs of the application. Response time of the sensor will of course depend on the selected packaging but less than 0.5 s is a typical value for a packaged sensor and about 1 ms for a bare sensor. A typical accuracy for this sensor is  $\pm 0.3^\circ\text{C}$  for a medical temperature range ( $20^\circ\text{C}$  to  $85^\circ\text{C}$ ) and  $\pm 1^\circ\text{C}$  for an industrial temperature range ( $-40^\circ\text{C}$  to  $300^\circ\text{C}$ ).

Another type of F-P temperature sensor is also available. This time, instead of material thermal dilatation, temperature dependent refractive index is rather used to change the OPD of the F-P sensor. A tiny chip of a semiconductor material with high thermal refractive index dependence and two semi-reflective surfaces constituting a F-P cavity is assembled at the tip of the lead optical fiber. This solid compact design is actually the smallest optical fiber temperature sensor available on the market ( $150\ \mu\text{m}$  square). Its sensitivity is about one order of magnitude lower than the capillary type temperature sensor but due to its extremely low thermal mass, its response time is better than  $5\ \mu\text{s}$  for a bare sensor which makes this sensor extremely interesting for fast temperature changes monitoring or for precise spatial point temperature mapping applications.

#### 2.4 Fiber Bragg grating temperature sensor

The fiber Bragg grating (FBG) temperature sensor technology [21] is quite different from the 3 previously cited ones. First instead of using multimode fiber (MMF), a low-cost single-mode fiber (SMF) is preferred (although MMF version of FBG is possible [22]). For SMF, the core is much smaller ( $8\text{-}10\ \mu\text{m}$ ) than for MMF ( $50\text{-}230\ \mu\text{m}$  or up to  $\sim 1$  mm for POF) to allow only one mode of light propagation. Such propagation mode is very interesting as SMF exhibits a narrower modal dispersion and has a higher bandwidth than MMF and also can retain the fidelity of each light pulse over a longer distance. Those are the reasons why SMF is now a standard in the telecommunication industry. Even though such fiber is usually cheaper in bulk, equipments for SMF are generally more expensive than for MMF. For instance, optical connectors need to have better mechanical tolerances to align correctly the smaller cores. Such connectors are also more sensitive to dust particles encountered



in industrial environments and that could unfortunately cover the whole fiber core.

Another important difference with the 3 previously cited OFS technologies resides in the fact that the sensor is actually written inside the fiber itself and it is not mounted at the tip of the fiber. It consists of a periodic modification of the SMF core refractive index with sections having a slightly higher index than the rest of the core. Several methods could be used to write the FBG, but the most common one involves core refractive index modification of a special germanium-doped silica fiber through intense UV laser illumination patterned by interferences or by masking technologies. Many types of grating structure are available (uniform, chirped, tilted...) but the most common are FBG with uniform index period ( $\Lambda$ ).

The fundamental principle behind FBG technology is Fresnel reflection as illustrated by Figure 4. The FBG is illuminated with a broadband infra-red (IR) light source (typically around 1510-1590 nm) and when light traveling in the core reaches the different refractive indices it may both reflect and refract at the interface. Part of the light is reflected depending on its wavelength, called the Bragg wavelength ( $\lambda_B$ ), which is defined by the equation:

$$\lambda_B = 2 \cdot n_e \cdot \Lambda \quad (5)$$

where  $n_e$  is the effective refractive index of the grating in the fiber core and  $\Lambda$  is the grating period. In SMF,  $n_e$  depends on the wavelength since only one propagation mode exists in such waveguide.

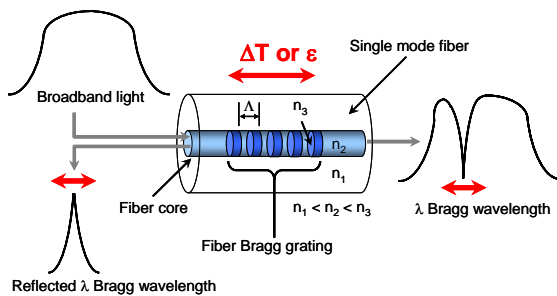


Figure 4: General principle of the FBG technology. The FBG is written into the core of a SMF. It consists of periodic slight variations of the core refractive index which affects the spectral response of the light passing through it. The FBG period  $\Lambda$  is affected by stretching due to temperature variation or strain impacting the reflected  $\lambda_B$  (red horizontal arrows).

FBG could be used in many ways in optical telecommunication systems (such as notch filter, multiplexers and demultiplexers...) but also it is widely used for sensing applications involving temperature but also strain/deformation, pressure depending on how the sensor is encapsulated. If the

grating period  $\Lambda$  is modified due to fiber thermal elongation or strain applied to the fiber, the Bragg wavelength  $\lambda_B$  will also be modified according to equation (6). Actually the relative shift of the Bragg wavelength ( $\Delta\lambda_B / \lambda_B$ ) due to an applied strain ( $\epsilon$ ) and a change in temperature ( $\Delta T$ ) is given by equation [23]:

$$\frac{\Delta\lambda_B}{\lambda_B} = C_S \cdot \epsilon + C_T \cdot \Delta T \quad (6)$$

where  $\lambda_B$  is the Bragg wavelength,  $C_S$  is the coefficient of strain,  $C_T$  is the coefficient of temperature.

An accurate determination with an optical spectrum analyzer (OSA) of the reflected narrow band around  $\lambda_B$  allows the evaluation of the actual combination of temperature and strain. In order to limit the strain contribution, special packaging care should be taken to ensure that the FBG is free from any constraints on its whole length (typically 5-10 mm). This is usually achieved by placing the FBG fiber inside a capillary with an internal diameter sufficiently large to avoid any contact between its surface and the sensing part of the fiber. This yields an encapsulated sensor with an outside diameter typically greater than 1 mm.

The Bragg wavelength would shift usually  $\sim 10$  pm/ $^\circ\text{C}$  which is sufficient to achieve an accuracy usually around  $\pm 0.5$ - $1^\circ\text{C}$  for a temperature range covering  $-40^\circ\text{C}$  to  $\sim 120^\circ\text{C}$ . Precision will naturally depend on the FBG interrogator performances as well as on the scan frequency (which could vary from 1 Hz to 1 kHz).

Since several FBG with slightly different grating period  $\Lambda$  could be written on the same SMF, multiple measuring points could be multiplexed and interrogated by the same channel, provided that  $\lambda_B$  dynamic overlaps are avoided by design. This is a great advantage offered by this quasi-distributed sensing technology. However since FBG interrogators and often packaged sensors are much more expensive than other cited technologies their use are practically limited to applications where cost is not a critical issue.

### 3 INDUSTRIAL APPLICATIONS

Fiber-optic temperature point-sensors have found several markets where they progressively became industry standards. Such niche markets were actually not correctly addressed by conventional electrical sensing technologies whereas OFS advantages made optical sensors the most reliable, simpler and sometimes even the cheaper solution. Some important examples are presented in this section.

### 3.1 Hot spot monitoring in transformers

One of the applications which made temperature OFS first commercial success is the hot spot monitoring in high-power transformers. Power transformers are always present as soon as electricity tension conversion is needed. Everybody is familiar with small power transformers used to charge their computer or cell phone, but much bigger ones have actually a very different design. They are present in areas where high-tension alternative current (110-1 200 kV) arriving from remote electricity power plants are converted into lower and less dangerous tension, typically 110 V or 220 V depending on the country.

The tension conversion is usually realized by induction between windings. The windings are made with copper wires separated with insulating layers. For the low-tension transformers of our day-to-day life the copper wires have simply a varnish as insulating layer, but for the high-tension transformers, higher dielectric properties are needed and dry cellulose paperboard is usually preferred. In order to maintain for decades the dielectric properties of the insulating paperboard, the assembled windings are dried and immersed in high-dielectric mineral oil and the whole assembly is sealed in a hermetic container. Even if the windings are low resistive, they always produce heat which increases with current power. For our low-tension transformers we could feel that heat which is easily dissipated. For high-tension transformers which cost several million USD, this is another story since heat generated is much more important and the consequence of overheating could be as catastrophic as an impressive explosion since they have a good source of electrical energy and a huge reservoir of easy-to-burn oil and paperboard...

Actually the life of a transformer (expected to be over 20-30 years) depends on the life of the insulation system. This life is defined by the chemical degradation processes which depend primarily on temperature and time. Other factors such as the presence of oxygen or moisture could be considered as accelerating the aging process. It is therefore very important to have a way to monitor not only the overall average temperature of the system but also it is essential to evaluate the temperature in strategic locations known as "hot spots". In those spots where temperature is more elevated than in the rest of the winding often due to design considerations, the degradation processes are locally accelerated, leading to aging of the cellulose though polymer chain breakdown generating byproducts such as glucose monomers further transformed to furanic compounds [24]. Those degradation products are partially soluble in the oil

reducing its dielectric properties not only locally but also in the whole transformer through oil convection processes.

Due to the presence of very high levels of EMI, *in situ* hot spot temperature measurement is impossible for conventional electrical sensors which are therefore confined in areas where they could be shielded such as at the top of the high-power transformer. Such measurements are not very precise and give only an idea of the thermal operating status of the transformer but no accurate evaluation of its windings hot spots. Those conventional methods have errors from inferring hot spots by trying to simulate or calculate the temperature versus directly measuring it. Inaccurate estimations could have drastic impact on the real life expectancy of the transformer as it decreases exponentially with the temperature of the hottest spot in the winding as shown in Figure 5: a slight 5-10°C increase of the hot spot reduces dramatically the life of the transformer, thus the returns on investments made for this very expensive utility.

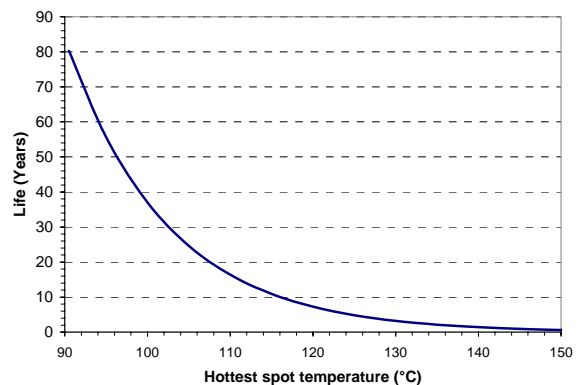


Figure 5: Minimum life expectancy for liquid-immersed transformer rated in accordance with IEEE Std C57.12.00-1993 (65°C average rise, 80°C hottest-spot rise). Graph adapted from IEEE C57.91-1995.

All penalties of conventional methods are overcome by *in situ* temperature measurements using fiber-optic point-sensors which could be installed directly into strategic points of the windings where hot spots are most suspected. Since such sensors are insensitive to the strong EMI and vibrating environments, they could perform where electrical counterparts are failing. The two OFS technologies which are now well accepted by the transformer industry are the fluorescence decay and the GaAs temperature sensors. Both types of sensors have been used with success in operating high-power transformers for now over 15 years. Their technical performances with a  $\pm 2^\circ\text{C}$  accuracy with low-speed

acquisition rate are satisfactory for this type of application.

Even though OFS are insensitive to strong EMI they could fail in this harsh environment if no attention is paid to the packaging of the sensor itself. For instance, the presence of air bubbles trapped into the sensor cable or tip assembly will be the source of partial discharges generated by the kV potential environment. Such discharges could lead with time to the sensor failure or worst, to a transformer failure since they may accelerate degradation of the dielectric medium. Thus specific care are taken to avoid such problems and all the cables used to protect the optical fibers are slotted or perforated (as shown on Figure 6) in order to allow ingress of insulating transformer oil into all possible voids of the sensor assembly.

A typical installation scheme of a power transformer is presented in Figure 7 with GaAs band-gap temperature sensing technology from *FISO Technologies*. The sensors are placed in different locations directly into the windings of the transformer during their manufacturing. Optical connectors are then plugged into a hermetic optical pass-through when the windings are inserted into the transformer casing. After a drying process involving heat and harsh solvents to remove as much as possible moisture and oxygen, the transformer casing

is sealed permanently. The temperature sensors are then connected to the signal conditioner using patch cords in order to record actual temperature data.

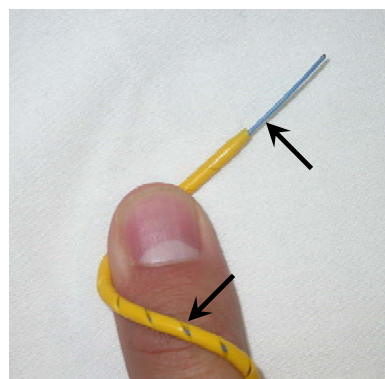


Figure 6: GaAs TPT-32 or TPT-62 temperature sensor from *FISO Technologies*. Slots (arrows) in the Teflon® cables are used to allow transformer immersing oil to fill all the voids of the sensor assembly.

Their use was originally very important for design and manufacturing steps of the transformers as they could give pertinent information that helped to reduce the temperature of hot spots and to improve utility general quality. They are also now often used

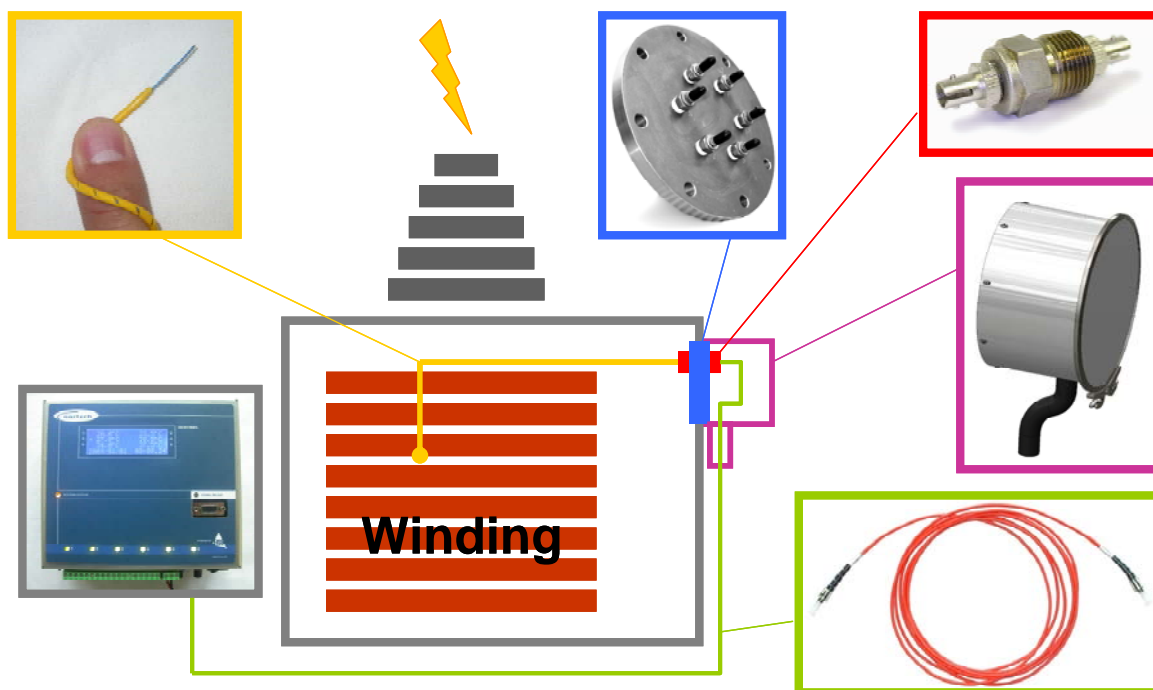


Figure 7: Typical installation scheme of OFS for hot spots monitoring in high-power transformers. Illustrated is the GaAs technology from *FISO Technologies*: Sensor (top left), *Easyplate*® (top center) *Easythrough*® (top right), *Easycover*® (middle right), patch-cord (bottom right) and 6 channels *Sentinel*® interrogator (bottom left).



as quality acceptance when the transformer is delivered to the final customer. As the transformer is in operation, the temperature OFS could be used as safety monitoring devices, as the OFS interrogator is often connected to relays and warning procedures could be activated when safety temperature limits are reached. With a better understanding of the actual temperature status of the transformer, the operator could even decide to use shortly the utility in overload mode in order to respond to a power peak demand, still preventing overheating and winding failure.

In the early times when OFS was introduced to this industrial application, their use was limited only to very high power (>100 MVA) and very expensive transformers. But with the OFS prices decrease of the last few years, this technology is now much more accessible to the whole industry and it started to be used for smaller transformers (20-100 MVA). More transformers are now instrumented with an increased number of sensors since redundancy enhances also their safety level. In the up-coming 2010 edition of the international standard IEC 60076-2 on power transformers, it will be recommended to instrument  $\geq 50$  MVA single-phase and  $\geq 20$  MVA 3-phase oil-filled transformers with at least 4 and 6-8 temperature OFS respectively, depending on their cooling system.

### 3.2 Semiconductor plasma etcher

In the semiconductor industry, plasma etcher is a key tool to pattern multi-layers trace paths for integrated circuits on silicon wafers using photolithography technologies. A plasma-assisted dry etch is often performed on masked wafers so that fine structured etching could be achieved at temperatures lower than possible without the help of the plasma. In normal procedure, the air is vacuumed and replaced by a process gas and a high-speed stream of glow discharge (plasma) is initiated using a high-frequency electric field (typically 13.56 MHz). The plasma could be used to grow silicon dioxide films on silicon wafers (oxygen plasma) or to remove silicon dioxide by using a fluorine or chlorine bearing gas. The process allows a reproducible, uniform etching of all materials used in silicon and III-V semiconductor technology. The performance of this tool is however highly dependent on pressure and temperature control. Temperature steps are included in the etching process and in order to increase throughput and uniformity there was a need for a temperature sensor that could perform in a plasma environment. Such harsh environment application with a limited number of measurement points on wafer holder was ideal for market penetration of temperature OFS.

### 3.3 Microwave chemistry and food applications

Microwave (MW) environment is also an area where temperature OFS have a clear advantage over electrical sensors as they are not affected by the EMI. In this area two major applications have been opportunities for the development of temperature OFS niche markets: microwave chemistry and food applications.

Microwave chemistry is the science of applying MW to chemical reactions [25-27]. As all electromagnetic radiations, MW radiation consists of two components: magnetic and electric field components. The MW electric field oscillates very quickly (at 2.45 GHz the field oscillates  $4.9 \times 10^9$  times per second) and this strong agitation is responsible for dielectric heating mechanism, either through molecular motion of ionic species (conduction mechanism) or rotation of dipolar species (dipolar polarization mechanism). This cyclic reorientation of molecules can result in an intense internal heating with heating rates of  $> 10^\circ\text{C/s}$  when MW radiation of 1 kW capacity source is used.

Such advantage combined with the fact that heating of chemicals is performed through their volume instead of through their surface provides interesting benefits over conventional ovens. Since all chemical reactions are dependent on temperature activation, reaction rates are accelerated and reaction conditions are usually milder. As a result, chemical yields are often higher as fewer by-products have time to be generated. Also, since heat is generated only inside the MW radiation-absorbing elements of the chemical reactor, lower energy is used. Finally different reaction selectivities could be achieved as MW radiation energy transfer depends on polarization properties and physical state of the chemicals involved in the reaction. Selective heating can also be achieved which is of particular interest for heterogeneous systems (comprising different substances or different phases) where MW energy is converted to heat by different amounts in different parts of the system. For binary systems such as polar and non-polar solvents, different temperatures could be achieved. For instance phase transfer reaction could be done with a temperature different for each phase, such as  $\sim 100^\circ\text{C}$  for water while maintaining only  $\sim 50^\circ\text{C}$  for chloroform.

Microwave chemistry began to gain popularity in the labs more than 20 years ago but really expanded in the industry with the introduction of temperature OFS in commercial MW reactor ovens. *In situ* temperature measurement during the MW heating allows a better control of MW activated chemical reactions since a feedback loop involving real-time temperature could be implemented in the process. F-P temperature sensors are commercially successful

for such applications, since sensor precision and response time are important specifications to consider together with the reasonable cost of the system. In order to be fully MW compatible, the optical sensor assembly has to be metal free, and if the sensor has to be connected inside the MW oven, this should include the optical connector where usually metal parts are present, for instance in the spring holding the ferrule. An example of a F-P temperature sensor designed by *FISO Technologies* for MW chemistry is presented in Figure 8. The whole sensor is protected by encapsulation inside chemically inert Teflon® tubing.

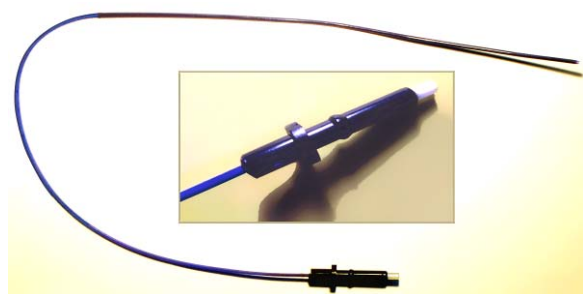


Figure 8: Example of a F-P temperature sensor designed by *FISO Technologies* for MW chemistry. Insert is a detail of the metal-free connector.

Another application involving temperature measurement in MW environment concerns food industry. Small MW ovens have now invaded our modern kitchens and are part of our busy day-to-day life where less time is available for cooking. As a result, this task is partially transferred to the food industry which now prepares various ready-to-serve meals which jump directly from the freezer to the MW oven to end few minutes later on the kitchen table.

Since MW heating depends on the chemical nature of the food and since the MW power is rarely uniform in the MW oven, it is very important to have a tool for real-time evaluation of the food temperature uniformity in order to know precisely how the heat is transferred from water-rich sections to others where MW energy is less absorbed. If the food disposition is not optimized, it is not rare to have hot-burning sections while others are still frozen, even if the food is rotated during the MW heating.

*FISO Technologies* is the only company which commercializes since several years OFS instrumented kitchen MW ovens which help food industry engineers to improve performances either of the MW heating program or of the food packaging itself, for instance by introducing honey-comb MW reflectors in strategic places of the packaging. In the

microwave station (MWS) shown in Figure 9, four to eight F-P temperature sensors (FOT-L) could be connected to the interrogator mounted on the top of the oven. The MWS interrogator is rotating with the MW plate in order to avoid sensors cables entanglement.



Figure 9: Commercial kitchen MW oven instrumented by *FISO Technologies* for multiple point-sensing with F-P temperature sensors.

### 3.4 Medical applications

More recently, optical temperature point-sensors have found many applications in the medical field. Again such sensors offer a solution in applications where electrical sensors do not perform correctly, mostly due to the presence of strong EMI.

For instance the very strong permanent magnetic field (typically 1.5-3 T) that is present in magnetic resonance imaging (MRI) is a true obstacle for metallic sensors which can not be used in such environment. Although MRI equipments are very expensive (~1-1.5 million USD for 1.5 T scanner) they are progressively invading the modern hospitals since they provide a unique non-invasive medical imaging tool used in radiology to visualize precisely in 2D or 3D detailed internal tissues as well as limited functions of the body.

Unlike the competitive and complementary traditional computational tomography (CT) imaging which uses ionizing radiations (X-rays) to acquire its images, MRI uses non-ionizing RF signals (strong magnetic fields) that are believed to be harmless to the patients (provided that they do not have MRI non compatible implants). As a result, the patients can undergo exams several times successively in the short term which is advantageous for close follow-up of some diagnosis or therapies. Also because MRI uses spin modifications induced in hydrogen nuclei, it is best suited for imaging soft tissues with many hydrogen nuclei and little density contrast, making it especially useful in neurological (brain), musculoskeletal, cardiovascular, and oncological (cancer) imaging.

Due to the construction of some MRI scanners which have small diameter bore (especially the old models since modern scanners have larger bores, up to 70 cm) and since imaging procedure could last up to 40 min during which patient should lie without moving in a very stressful noisy clicking and beeping environment (up to 120 dB equivalent to a jet engine at take-off [28]), for those reasons, some MRI patients suffer from claustrophobia and discomfort and in many cases they have to be sedated. This is particularly the case if MRI is used during surgery (such as for instance for brain surgery) or when small children have to undergo this imaging procedure.



Figure 10: Example of medical OFS assembly developed by *FISO Technologies* for skin surface temperature sensing of patient during MRI procedure. The diameter of the blue cables is 3 mm.

It is important during patient sedation to monitor their vital signs such as temperature, in order to be able to react and interrupt the procedure if some abnormal situation is encountered. Some examples of skin surface temperature F-P sensors used during MRI procedure are presented in Figure 10.

Other applications of optical point-sensors in MRI field concern for instance MRI safety evaluation of implants, medical devices or materials. Under very strong magnetic fields, even non-ferromagnetic materials could experience some effects depending on the design. In some cases local elevation of temperature could be recorded and provide useful information to engineers. Minimally invasive temperature OFS insensitive to magnetic fields are successfully used to find hot spots generated in MRI environment. They could also be used for improving the design of custom coils that are used for imaging specific parts of the human body.

Optical temperature point-sensors could be used as well in medical therapies such as hyperthermia therapy which is used to help treating some cancers. Hyperthermia therapy is a medical treatment consisting of exposing body tissues to high temperature to damage and kill cancer cells or to make them more sensitive to the effects of radiations and certain anti-cancer drugs. The problem of this

therapy is to localize and control temperature elevation and heat transfer to limit deleterious effects to tumor cells without damaging too much healthy cells and without elevating too much the whole body temperature (normally around 37.6°C, 42°C being maximum temperature compatible with life). Fortunately tumor cells are disorganized and have a compact vascular structure which makes them have more difficulties dissipating heat. In moderate hyperthermia, a local temperature of 40-43°C is usually generated to kill the cells. Very high temperatures (above 50°C) are used for ablation of some tumors which are so to speak literally burned (thermal ablation).

Miniaturization of heat treatment is actually quite important: the smaller the area that is heated and the shorter the treatment time with associated the lower the side effects. Depending on the location of the tumor, heat could be applied to the surface of the body, inside normal body cavities or through tissues using needles or probes. Several sources are used to generate heat tissues locally and among them MW and RF sources offer interesting advantages. However they make real-time temperature feedback control difficult due to the presence of EMI... unless OFS are utilized. The use of temperature OFS is furthermore recommended when the hyperthermia therapy is done under MRI which could be used as a way for correctly positioning the heating elements on the right spot of tumor cells.

Since heat is transferred and dissipated in neighbor tissues, having information on thermal distribution within the surrounding tissues is also very useful. This is the reason why equally spaced temperature optical point-sensors integrated into a small instrumented catheter as shown in Figure 11 provide an interesting tool helping the therapy.

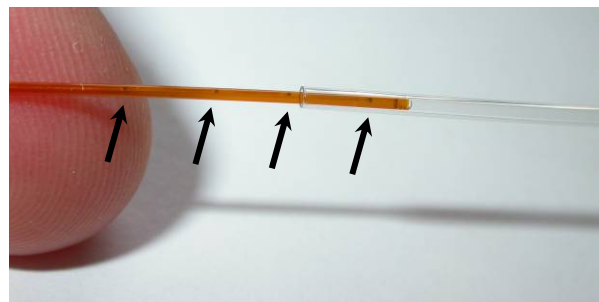


Figure 11: Example of an 840 µm OD instrumented catheter designed by *FISO Technologies* for multiple point temperature sensing compatible with RF/MW hyperthermia therapy or thermal ablation. Arrows show the positions of four GaAs sensors.

#### 4 CONCLUSION

Emergence of commercial fiber-optic temperature sensors in the industrial world was originally possible due to the unique sensing advantages provided by such technologies. They could perform better in many environments where other sensors fail: mainly environments with any type of strong EMI, with fire or explosion risks or simply with harsh temperature or chemical conditions. Among all the possible technologies developed by academic research, only very few ended to actual commercial success. Unfortunately OFS are still more expensive than conventional technologies and can therefore compete only in few niche-markets where they have technological advantages. As a result, the four robust temperature point-sensing OFS technologies which are presently successfully commercialized are fluorescence decay, GaAs band-gap variation, F-P interferometry and FBG. Each of them has its own advantages and limitations which make them suitable for various industrial applications as presented in this paper.

Over years passed sensing temperature in the “real world”, OFS proved that they have unique and reliable performances which make them players impossible to circumvent when safety or robustness are concerned. With the progresses made by the OFS companies for pushing those technologies to their limits while decreasing as much as possible the selling price, one can guess that new niche-markets will emerge or expand at it is presently the case for hot spot monitoring in power transformers as explained in this paper. The fact also that such technology is now better known and well accepted in the scientific and engineer communities will contribute for sure to better market opportunities as they will be more and more tested in new applications...

#### References

- [1] D. A. Krohn, *Fiber Optic Sensors: Fundamentals and Applications*, Instrument Society of America (Pub.), Research Triangle Park, NC, USA, 2nd ed., ISBN 0-55617-010-6, 1992
- [2] J. M. López-Higuera, *Handbook of Optical Fibre Sensing Technology*, John Wiley & Sons (Pub.), Chichester, West Sussex, England, ISBN 0-471-82053-9, 2002
- [3] W. J. Bock, I. Gannot and S. Tanev, *Optical Waveguide Sensing and Imaging*, Springer (Pub.), Dordrecht, The Netherlands, ISBN 978-1-4020-6951-2, 2006
- [4] S. Yin, P. B. Ruffin and F. T. S. Yu, *Fiber Optic Sensors*, CRC Press (Pub.), Taylor & Francis Group, Boca Raton, FL, USA, 2nd ed., ISBN 978-1-4200-5365-4, 2008
- [5] D. Schaafsma, G. Palmer and J. H. Bechtel “Fiber optic temperature sensors for medical applications” *Optical Fibers and Sensors for Medical Applications III, Proc. SPIE*, **Vol. 4957**, pp. 162-169, 2003
- [6] É. Pinet, C. Hamel, B. Glišić, D. Inaudi, and N. Miron, “Health monitoring with optical fiber sensors: from human body to civil structures”, *Proc. SPIE*, **Vol. 6532**, pp. 653219-1 to 653219-12, 2007
- [7] É. Pinet, “Medical applications / Saving lives”, *Nature Photon. Tech. Focus* (special edition on fiber-optic sensors), **Vol. 2**, pp. 150-152, 2008
- [8] D. A. Krohn, “Temperature sensors” in *Fiber Optic Sensors: Fundamentals and Applications*, Instrument Society of America (Pub.), Research Triangle Park, NC, USA, 2nd ed., ISBN 0-55617-010-6, **Chap. 7**, pp. 117-136, 1992
- [9] H. Aizawa, N. Ohishi, S. Ogawa, T. Katsumata, S. Komuro, T. Morikawa and E. Toba, “Fabrication of ruby sensor probe for the fiber-optic thermometer using fluorescence decay”, *Rev. Sci. Instrum.*, **Vol. 73**, pp. 3656-3658, 2002
- [10] G. Paez and M. Strojnik, “Erbium-doped optical fiber fluorescence temperature sensor with enhanced sensitivity, a signal-to-noise ratio, and a power ratio in the 520-530- and 550-560-nm bands”, *Appl. Opt.*, **Vol. 42 (16)**, pp. 3251-3258, 2003
- [11] J.L. Wu, “A high-temperature sensor based fluorescence lifetime”, *Proc. SPIE*, **Vol. 6280**, pp. 0347-0352, 2006
- [12] T. Katsumata, “Characteristics of Ti-doped sapphire for fluorescence thermo-sensor”, *Int. Conf. Control Automat & Syst.*, **Vol. 1-6**, pp. 1025-1028, 2007
- [13] A. Babnik, A. Kobe, D. Kuzman, I. Bajsič and Možina, “Improved probe geometry for fluorescence-based fibre-optic temperature sensor”, *Sensors and Actuators A*, **Vol. 57**, pp. 203-207, 1996
- [14] H. Chungai and W. Yutian, “Digital signal processing for fluorescence-based fiber-optic temperature sensor”, *Proc. SPIE*, **Vol. 4920**, pp. 98-100, 2002
- [15] M. R. Brozel and G. E. Stillman (Eds.), “Properties of Gallium Arsenide”, 3rd Ed. *Institution of Electrical Engineers*, London, 1996
- [16] É. Pinet “Fabry-Pérot fiber-optic sensors for physical parameters measurement in challenging

- conditions”, *Journal of sensors*, Vol. 2009, Article ID 720980, 9 p., 2009, available at <http://www.hindawi.com/journals/js/2009/720980.html>
- [17] C. Belleville and G. Duplain, “Fabry-Perot optical sensing device for measuring a physical parameter”, *US Patents* #5,202,939 1993 & #5,392,117, 1995
- [18] [www.fiso.com](http://www.fiso.com)
- [19] R. Van Neste, C. Belleville, D. Pronovost and A. Proulx, “System and method for measuring an optical path difference in a sensing interferometer”, *US patent*, #2004/0075841 A1, 2004
- [20] M. Chavko, W.A. Koller, W.K Prusaczyk and R.M. McCarron, “Measurement of blast wave by miniature fiber optic pressure transducer in the rat brain”, *J. Neurosci. Meth.*, **Vol. 159 (2)**, pp. 227-281, 2007
- [21] L. Zhang, W. Zhang and I. Bennion, “In-fiber grating optic sensors” in *Fiber Optic Sensors*, CRC Press (Pub.), Taylor & Francis Group, Boca Raton, FL, USA, 2nd edition, ISBN 978-1-4200-5365-4, **Chap. 4**, pp. 109-162, 2008
- [22] S. Yin, C. Zhan and P.B. Ruffin, “Femtosecond laser-inscribed harsh environment fiber Bragg grating sensors” in *Fiber Optic Sensors*, CRC Press (Pub.), Taylor & Francis Group, Boca Raton, FL, USA, 2nd edition, ISBN 978-1-4200-5365-4, **Chap. 5**, pp. 163-200, 2008
- [23] A. Othonos and K. Kalli, “Fiber Bragg gratings: Fundamentals and applications in telecommunications and sensing”, Artech House, ISBN 0890063443, 1999
- [24] D.H. Shroff and A.W. Stannet, “A review of paper aging in transformers”, *IEEE Proc.*, **Vol. 132 (6)**, part C, Nov 1985
- [25] A. Loupy Ed., “Microwave in organic synthesis”, Wiley-VCH, Weinheim, 2006
- [26] D. Bogdal, “Microwave-assisted organic synthesis, One hundred reaction procedures”, *Tetrahedron Organic Chemistry*, **Vol. 25**, Elsevier Ltd (Pub.), Oxford, UK, 2005
- [27] A. de la Hoz, A. Diaz-Ortiz and A. Moreno, “Microwaves in organic synthesis. Thermal and non-thermal microwave effects”, *Chem. Soc. Rev.*, **Vol. 34 (2)**, pp. 164-178, 2005
- [28] D.L. Price, J.P. de Wilde, A.M. Papadaki, J.S. Curan and R.I. Kitney, “Investigation of acoustic noise on 15 MRI scanners from 0.2 T to 3 T”, *J. Magn. Res. Imag.*, **Vol. 13 (2)**, pp. 288-293, 2001